Structure and enzymatic activity of laser immobilized ribonuclease A

ARTICLE *in* JOURNAL OF MATERIALS SCIENCE · JUNE 2014

Impact Factor: 2.37 · DOI: 10.1007/s10853-014-8136-0

9 AUTHORS, INCLUDING:

Andrei Popescu

National Institute for Laser, Plasma and Ra…

47 PUBLICATIONS **237** CITATIONS

SEE PROFILE

Enikö György

National Institute for Laser, Plasma and Ra…

117 PUBLICATIONS **1,326** CITATIONS

SEE PROFILE

J Mater Sci (2014) 49:4371–4378
DOI 10.1007/s10853-014-8136-0

Structure and enzymatic activity of laser immobilized ribonuclease A

C. Popescu · A. C. Popescu · I. Iordache · M. Motoc · D. Pojoga · A. Simon-Gruita · N. Constantin · G. Duta Cornescu · E. Gyorgy

Received: 13 December 2013 / Accepted: 27 February 2014 / Published online: 13 March 2014

Abstract Ribonuclease A (RNase A) enzyme was immobilized on solid holders by matrix-assisted pulsed laser evaporation (MAPLE) technique. The experiments were performed inside a stainless steel irradiation chamber. A UV KrF* ($\lambda = 248$ nm, $\tau_{FWHM} \cong 25$ ns, $\nu = 10$ Hz) excimer laser source was used for irradiations. Surface morphology, molecular structure, and enzymatic activity of laser transferred RNase A samples were investigated as a function of RNase A concentration in the frozen composite MAPLE targets. Surface morphology and thickness of the immobilized enzyme were investigated by atomic force microscopy, scanning electron microscopy, and surface profilometry. The molecular structure of the laser transferred RNase A was determined by Fourier transform infrared spectroscopy. The enzymatic activity of RNase A after immobilization was tested through ribonucleic acid removal from deoxyribonucleic acid (DNA) extract solutions isolated from plant and animal tissues. A molecular method based on polymerase chain reaction was used to investigate the functional properties of DNA extracts treated with laser immobilized RNase A.

C. Popescu · A. C. Popescu · I. Iordache · M. Motoc · E. Gyorgy
National Institute for Lasers, Plasma and Radiations Physics, P. O. Box MG 36, 77125 Bucharest, Romania

D. Pojoga · A. Simon-Gruita · N. Constantin · G. Duta Cornescu
Department of Genetics, Faculty of Biology, University of Bucharest, 060101 Bucharest, Romania

E. Gyorgy (✉)
Consejo Superior de Investigaciones Científicas, Instituto de Ciencia de Materiales de Barcelona (CSIC-ICMAB), Campus UAB, 08193 Bellaterra, Spain
e-mail: egyorgy@icmab.es

Introduction

Ribonuclease A (RNase A) is a single subunit enzyme with a molecular weight of ~13.7 kDa. Its natural abundance in the bovine pancreas and its high conformational stability, made RNase A an ideal model system for studies concerning protein structure and functions [1]. One of the most important practical uses of RNase A is the removal of ribonucleic acid (RNA) from deoxyribonucleic acid (DNA) extract solutions [2–4]. As known, during DNA isolation processing, RNA is co-purified with genomic DNA. Its elimination from DNA extracts represents a mandatory subsequent step since RNA contamination of DNA isolates may prevent accurate and effective DNA sequencing. As a consequence, the addition of RNase A is critical to obtain pure DNA extracts. However, after RNA degradation, RNase A has to be eliminated from the decontaminated DNA solutions. Immobilization of RNase A onto solid materials surfaces would allow for its easy removal from the solutions, permitting also a better control over the enzymatic reactions.

RNase enzymes are also known as therapeutic biomaterials, because their toxicity for cancer cells [5, 6], promote angiogenesis [7], have antiviral [8] and antimicrobial activity [9]. Therefore, the immobilization of RNase enzymes on solid three-dimensional biocompatible and bioresorbable materials surfaces could represent new solutions also in medical therapy [10–12]. The process is known as surface-mediated drug delivery and implies the release of therapeutic molecules from the surface of a biomaterial, usually an implant, to the adjacent tissues [13–15]. However, organic complex biomolecules immobilization onto solid surfaces is not an easy task. It is well known that significant changes of the initial material composition can take place during the immobilization

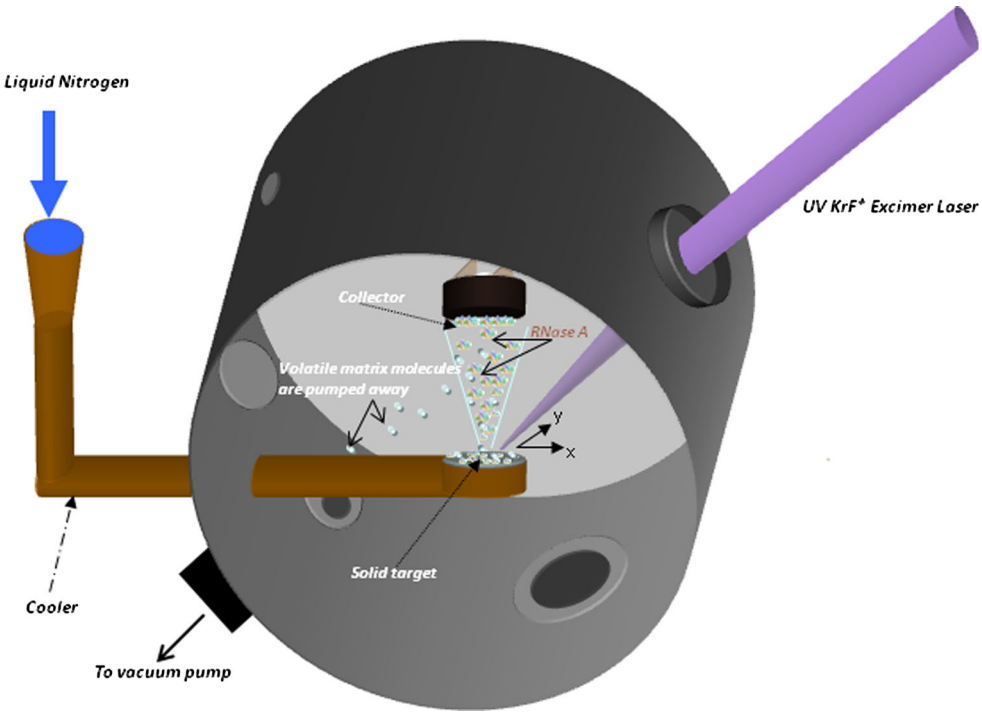

Fig. 1 MAPLE experimental set-up

process, leading to alterations of functional properties such as stability and biological activity, restraining the practical applications of the synthesized structures [16].

Matrix-assisted pulsed laser evaporation (MAPLE) is an immobilization method developed for the deposition of complex organic molecules in form of thin films [17, 18]. Methods involving laser radiation ensure the accurate control of the amount of material evaporated and deposited on a substrate surface by the number and/or intensity of the laser pulses [19]. Moreover, laser processes could overcome the most common drawbacks of conventional immobilization techniques, which are mostly multi-step procedures of high cost, require the presence of chemical substances as well as specific pre-treated substrate materials.

In MAPLE the material to be deposited is dissolved or suspended in a volatile solvent which is vaporized, carrying the organic molecules toward a substrate surface. The solvent material is usually selected to be highly absorbing at the incident laser wavelength, reducing the thermal damage on the material of interest. However, it was recently demonstrated that MAPLE process is effective in the opposite situation as well, i.e., for materials with high absorption at the laser wavelength, embedded in solvents transparent to the laser radiation [20–25].

In this study, we investigated the interdependence between RNase A concentration in the frozen composite MAPLE targets and morphology, molecular structure, as well as enzymatic activity of laser transferred RNase A. The immobilized RNase A enzymatic activity was tested using DNA extract solutions containing RNA contamination traces. The quality of purified DNA extracts was further investigated by a polymerase chain reaction (PCR) based method using random decameric primers.

Experimental details

The experiments were performed inside a stainless steel irradiation chamber, using pulsed UV KrF* ($\lambda = 248$ nm, $\tau_{FWHM} \cong 25$ ns, $\nu = 10$ Hz) COMPexPro excimer laser source. The composite targets were prepared by dissolving RNase A in a buffer HEPES–NaOH, pH 7.5 solvent, at three different concentrations: 0.2, 0.5, and 1 wt%. The obtained solutions were frozen in liquid nitrogen inside a double-wall target holder mounted in the irradiation chamber (Fig. 1). The solutions were kept frozen during the laser irradiation experiments. The MAPLE workstation was a commercial one, purchased from Surface Systems & Technology GmbH &Co KG, (Hückelhoven, Germany).

Before each experiment, the irradiation chamber was evacuated down to a residual pressure of 1.6×10^{-2} Pa. This pressure value was maintained during the RNase A transfer process. The laser fluence incident on the targets' surface was fixed at 0.5 J/cm^2. The laser beam incidence angle on the target surface was 45°. To avoid significant morphological changes during irradiation, the laser beam scanned the targets' surface at a constant velocity of 2 mm/s. 2×10^4 subsequent laser pulses were applied during each laser immobilization experiment. RNase A was immobilized onto 0.5×0.5 cm^2 SiO_2 glass substrates, placed plan-parallel to the target surface

at a separation distance of 5 cm. During MAPLE deposition, the substrates were kept at room temperature.

The surface morphology of the immobilized RNase A was investigated by scanning electron microscopy (SEM) and atomic force microscopy (AFM) in acoustic (dynamic) configuration. SEM investigations were conducted with a FEI Inspect S electron microscope. The AFM analyses were performed with a PicoSPM Molecular Imaging apparatus. The obtained data were studied with Mountains Map software from Digital Surf. The thickness of immobilized RNase A was assessed by surface profilometry, using Stylus Profiler XP 2 from Ambios Technology with 1.5 Å vertical resolution. The chemical composition and bonding states between the elements were studied by Fourier transform infrared spectroscopy (FTIR) in the 4000–500 cm^{-1} wavenumber range, using a 4 cm^{-1} resolution Shimadzu 8400S Spectrum apparatus.

The enzymatic activity of the laser immobilized RNase A was tested through decontamination experiments, consisting of removal of RNA traces from genomic DNA extract solutions isolated from plants (*Hippophae rhamnoides*) and animals (*Drosophila melanogaster* and *Mus musculus—BalbC mouse*). DNA extractions were performed with Wizard Genomic DNA purification Kit (Promega) for *Hippophae rhamnoides* and *Drosophila melanogaster*. LiCl protocol was used for DNA extraction from *Mus musculus—BalbC mouse*. The efficiency of RNA removal from the DNA extract solutions was determined by: (i) 1 % agarose gel electrophoresis in 1× TBE buffer at 80 V and (ii) spectrophotometry using nanodrop ASP 280 (GE Healthcare Life Sciences) measuring the absorbance values of the DNA extract solutions at 260 nm, A_{260}, and at 280 nm, A_{280}, before and after RNase A treatment. This last method allows for the quantitative analyses of RNase A activity since the decrease of A_{260}/A_{280} ratio is proportional to the RNA removal from the DNA extract solutions.

The RNase A treated DNA extracts solutions were tested in an amplification protocol in order to establish the suitability of the solutions for future use in molecular experiments. The RAPD reaction (Random Amplified Polymorphic DNA) (Ercisli 2008) used two decameric primers: OPD-18 (GAG AGC CAA C) and OPC-11 (AAA GCT GCG G) (Bio Basic Inc.). PCR program was 5 min/95 °C initial denaturation, followed by 45 cycles of 1 min at 95 °C, 1 min at 36 °C and 2 min at 72 °C and a final extension step of 10 min at 72 °C. The amplicons, representing randomly amplified DNA fragments, were visualized in 2 % agarose gel electrophoresis.

Results and discussion

Morphological investigations

The SEM images of laser immobilized RNase A using frozen composite MAPLE targets with 0.2 and 0.5 wt% RNase A concentrations are presented in Fig. 2. As can be observed, for these RNase A concentrations the laser transferred enzyme does not form a continuous layer. At 0.2 wt% RNase A concentration in the composite target (Fig. 2a, b), the deposited structures consist of individual structures, with dimensions of few μm having round as well as elongated, 5–7 μm length, rod-like shapes. With the increase of the enzyme concentration from 0.2 to 0.5 wt% in the composite targets (Fig. 2c, d), both the dimensions and the density of the particles increase. The rods are randomly oriented on the substrate surface forming dendritic islands (Fig. 2d). As can be observed in Fig. 2b and d, the circular, ring-shape as well as rod-like structures are formed by small particles. Ring-shape features, concentrating the material at their edges as well as inter-connected line structures, formed by tens of nm sized particles were observed also in case of CdSe/ZnS core–shell nanoparticles immobilized on SiO_2 glass substrates by UV-MAPLE technique, using highly absorbing solvent at the incident laser radiation [26, 27]. Until certain extent similar circular, ring-shape structures were identified in case of MAPLE deposition of carbon nanopearls [28], using solvents with high absorption at the incident laser radiation. For solvents with low absorption at the laser radiation, as in our experiments, the circular features were present, although both their number and dimensions were reduced. The effect was attributed to expulsion of liquid droplets from the targets which hit the surface and evaporate, leaving behind the material around their edges.

By doubling the RNase A content in the target to 1 wt%, the laser transferred material formed a continuous and compact thin film, as confirmed by AFM investigations (Fig. 3a). We also presented in Fig. 3b the surface profile corresponding to the line marked in the AFM image. As can be observed in the AFM image and surface profile, the mean diameter of the nanoparticles is around 100 nm, having a quite homogeneous size distribution. Larger particles, with dimensions of a few hundreds of nm can be also detected.

The thickness of the samples was determined by surface profilometry (Fig. 4). To this purpose, five surface profiles were registered for each sample corresponding to different locations. The measured thickness values for the samples obtained at 0.2 and 0.5 wt% RNase A concentrations increase from about 150 to 350 nm (Fig. 4a, b). However, we would like to recall that these samples are constituted of discontinuous structures. As a consequence, the profiles correspond to the heights of the individual particles. The increase of the concentration to 1 wt% leads to the formation of a continuous film with a thickness of around 350 nm (Fig. 4c).

Characterization of chemical composition

The molecular structure of the laser immobilized RNase A was investigated by FTIR spectroscopy (Fig. 5). The

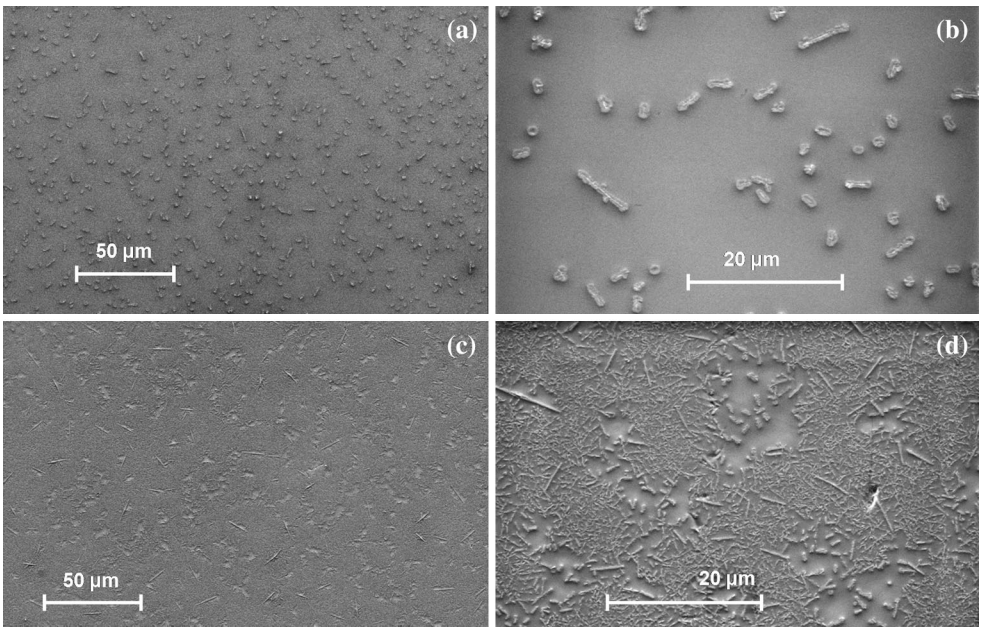

Fig. 2 SEM images of the immobilized RNase A obtained by the irradiation of frozen composite MAPLE targets containing (**a**, **b**) 0.2 wt% and (**c**, **d**) 0.5 wt% RNase A concentrations

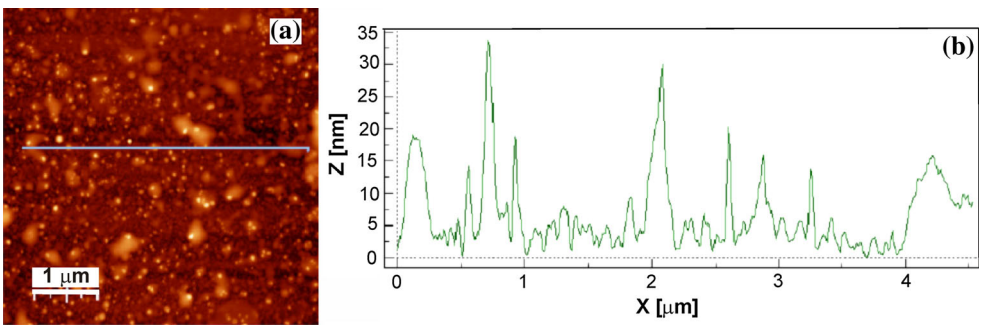

Fig. 3 **a** AFM images of the immobilized RNase A obtained by the irradiation of 1 wt% RNase A frozen composite target and **b** surface profile corresponding to the line marked in the AFM image

immobilized RNase A spectrum (Fig. 5a) was compared with the spectrum of the initial RNase A enzyme solution used for the preparation of the MAPLE targets (Fig. 5b) as well as to the enzyme solution collected from the target holder after the laser immobilization experiments, further referred as final enzyme solution (Fig. 5c). To this aim, drop-cast samples were prepared using the initial and final solutions. The spectrum of the transferred enzyme is similar to that of the initial solution as well as to that of the final solution. It is composed by the characteristic bands of the RNase A: (i) the amide A band centered around 3400 cm^{-1} due to N–H stretching vibrations, (ii) the band at 1654 cm^{-1} corresponding to the amide I region governed by C=O and C–N stretching vibrations, (iii) the band at 1534 cm^{-1} assigned to tyrosine amino acid residues, (iv) the band at 1464 cm^{-1} of the amide II region attributed to in-plane N–H bending as well as C–N stretching vibrations, and (v) the band at around 1400 cm^{-1} which could correspond to the amide III region [29–31]. The bands intensity of the MAPLE immobilized enzyme is lower as the film is about five times thinner as compared to the drop-cast samples. The obtained results indicate that molecular composition and structure of the enzyme are preserved throughout the MAPLE transfer process.

Enzymatic activity of laser immobilized RNase A

Isolation protocols provided DNA extract solutions with concentrations around 1,000 μg/mL for plants (*Hippophae rhamnoides*) and 3,000 μg/mL for animals (*Drosophila melanogaster* and *Mus musculus—BalbC mouse*). Due to these high DNA concentration values no enzymatic activity was detected for laser immobilized RNase A samples, or for the initial or final RNase A solutions. Thus, serial dilutions from the DNA extracts were made until reaching a DNA concentration of around 100 μg/mL. The obtained solutions were used to test the enzymatic activity of RNase A by agarose gel electrophoresis (Figs. 6, 7) and spectrophotometry (Table 1).

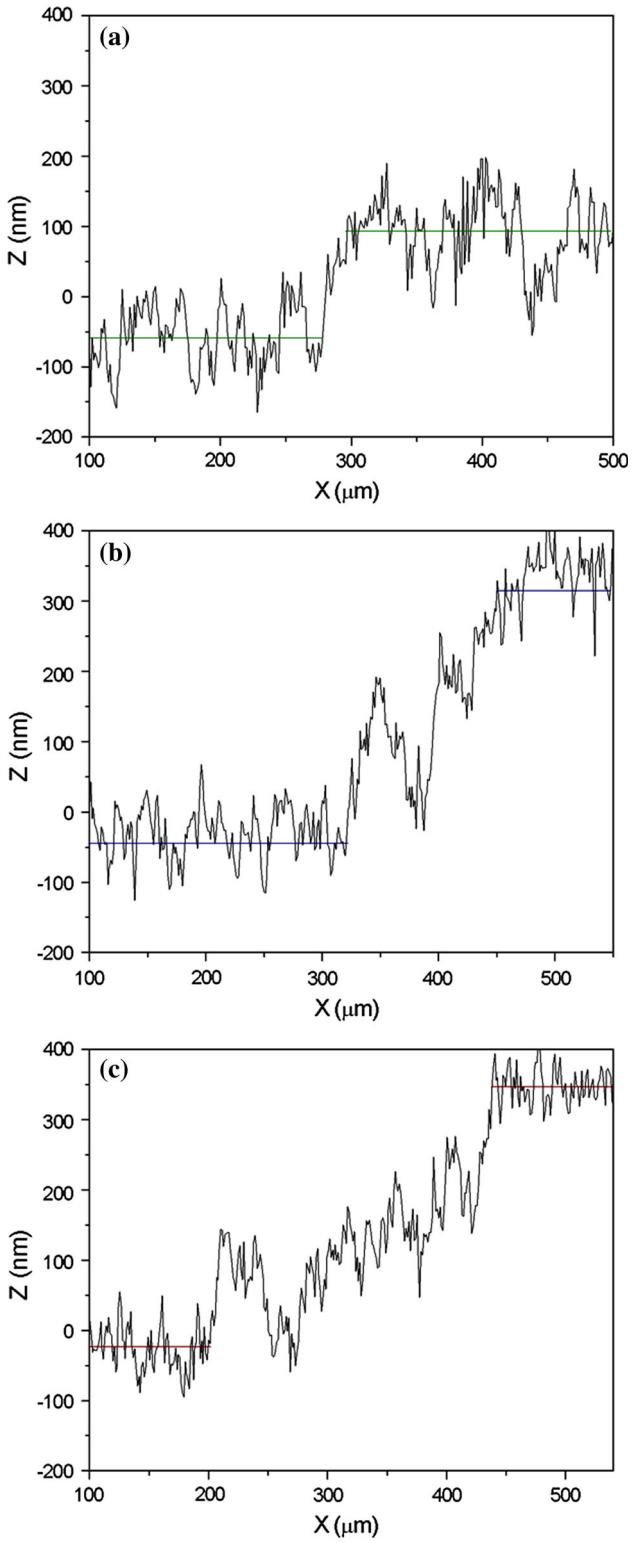

Fig. 4 Thickness of the immobilized RNase A obtained by the irradiation of frozen composite targets containing **a** 0.2, **b** 0.5, and **c** 1 wt% RNase A concentrations

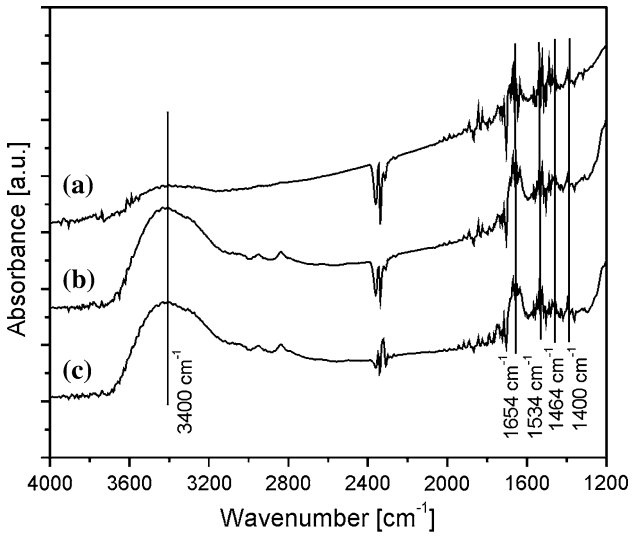

Fig. 5 FTIR images of (*a*) laser immobilized RNase A obtained by the irradiation of 1 wt% frozen composite RNase A target, and the drop-cast samples of (*b*) initial and (*c*) final MAPLE target solutions of RNase A in buffer HEPES–NaOH, pH 7.5

Lanes 1, 5, and 9 illustrate untreated DNA extract solutions isolated from *Hippophae rhamnoides* (Fig. 6) and from *Mus musculus—BalbC mouse* (Fig. 7). The solution from the lanes were submitted to treatment with RNase A, in form of initial solution used as targets in the MAPLE experiments (lanes 2, 6, and 10), immobilized on SiO_2 glass substrates (lanes 3, 7, and 11), and final solution extracted from the target holder after the MAPLE experiments (lanes 4, 8, and 12). Lanes 1, 5, and 9 served as starting DNA solution submitted to RNA decontamination experiments with 0.2, 0.5, and 1 wt% RNase A, respectively. The RNA contamination in the DNA solutions (lanes 1, 5, and 9 in Figs. 6, 7) appears typically like a diffuse cloud toward the bottom part of the lanes during agarose gel electrophoresis [32]. As can be observed in Figs. 6 and 7, RNA concentration is significantly reduced when the DNA extracts are treated with RNase A initial and final MAPLE target solutions, lanes 2 and 4, 6 and 8, 10 and 12 becoming more transparent as compared to their untreated counterparts (lanes 1, 5, and 9, respectively). However, in case of immobilized enzyme (lanes 3, 7, and 11) partial RNA decontamination takes place, and only at the highest, 1 wt% RNase A concentration (lanes 11 in Figs. 6, 7).

Spectrophotometry analyses proved to be more sensitive than agarose gel electrophoresis in revealing the reduction of RNA concentration in the DNA extracts after RNase A administration. The ratio between the absorbance values at 260 and 280 nm wavelengths (A_{260}/A_{280}) is suitable to

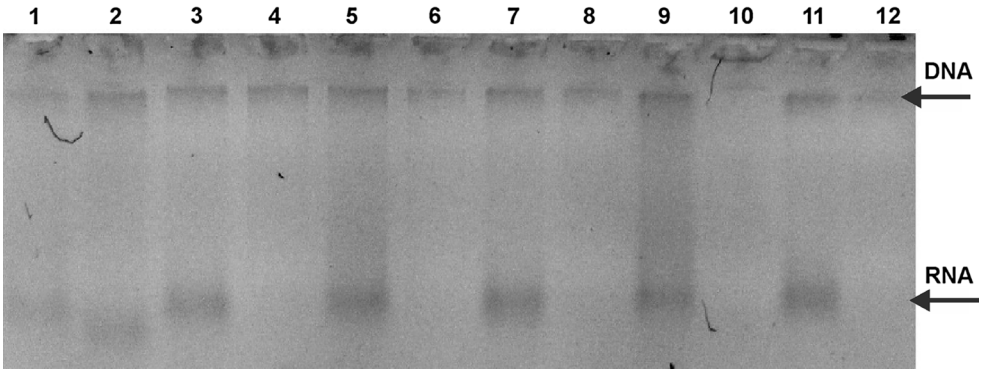

Fig. 6 DNA extracts isolated from *Hippophae rhamnoides* for *1*. untreated DNA extract, *2*. DNA extract treated with 0.2 wt% RNase A initial MAPLE target solution, *3*. DNA extract treated with immobilized RNase A from the 0.2 wt% RNase A concentration MAPLE target, *4*. DNA extract treated with 0.2 wt% RNase A final MAPLE target solution, *5*. untreated DNA extract, *6*. DNA extract treated with 0.5 wt% RNase A initial MAPLE target solution, *7*. DNA extract treated with immobilized RNase A from the 0.5 wt% RNase A concentration MAPLE target, *8*. DNA extract treated with 0.5 wt% RNase A final MAPLE target solution, *9*. untreated DNA extract, *10*. DNA extract treated with 1 wt% RNase A initial MAPLE target solution, *11*. DNA extract treated with immobilized RNase A from the 1 wt% RNase A concentration MAPLE target, and *12*. DNA extract treated with 1 wt% RNase A final MAPLE target solution

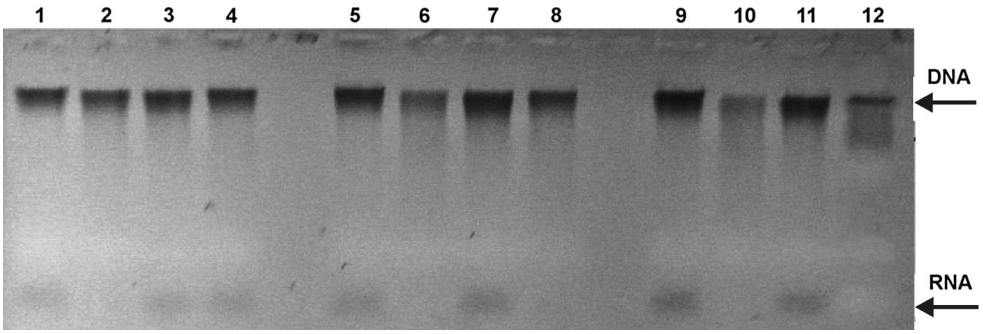

Fig. 7 DNA extracts isolated from *Mus musculus—BalbC mouse* for *1*. untreated DNA extract, *2*. DNA extract treated with 0.2 wt% RNase A initial MAPLE target solution, *3*. DNA extracts treated with immobilized RNase A from the 0.2 wt% RNase A concentration MAPLE target, *4*. DNA extracts treated with 0.2 wt% RNase A MAPLE target final solution, *5*. untreated DNA extracts, *6*. DNA extracts treated with 0.5 wt% RNase A initial MAPLE target solution, *7*. DNA extracts treated with immobilized RNase A from the 0.5 wt% RNase A concentration MAPLE target, *8*. DNA extracts treated with 0.5 wt% RNase A final MAPLE target solution, *9*. untreated DNA extracts, *10*. DNA extracts treated with 1 wt% RNase A initial MAPLE target solution, *11*. DNA extracts treated with immobilized RNase A from the 1 wt% RNase A concentration MAPLE target, and *12*. DNA extracts treated with 1 wt% RNase A final MAPLE target solution

Table 1 A_{260}/A_{280} ratios of genomic DNA extracts isolated from plants (*Hippophae rhamnoides*) and animals (*Drosophila melanogaster* and *Mus musculus—BalbC mouse*) before (I) and after (II) RNase A treatment

RNase A	RNase A wt% in the MAPLE target	*Balb C mouse*			*Drosophila melanogaster*			*Hippophae rhamnoides*		
		A_{260}/A_{280} (I)	A_{260}/A_{280} (II)	A_{260}/A_{280} (I) − A_{260}/A_{280} (II)	A_{260}/A_{280} (I)	A_{260}/A_{280} (II)	A_{260}/A_{280} (I) − A_{260}/A_{280} (II)	A_{260}/A_{280} (I)	A_{260}/A_{280} (II)	A_{260}/A_{280} (I) − A_{260}/A_{280} (II)
I	0.5	1.913	1.719	0.194	1.353	1.216	0.137	1.346	1.290	0.056
Im	0.5	1.914	1.884	0.030	1.339	1.335	0.004	1.371	1.333	0.038
	1	1.915	1.841	0.074	1.368	1.335	0.033	1.327	1.203	0.124
F	0.5	1.928	1.757	0.171	1.340	1.216	0.124	1.361	1.330	0.031

I initial RNase A solution, *Im* immobilized RNase A, *F* final RNase A solution

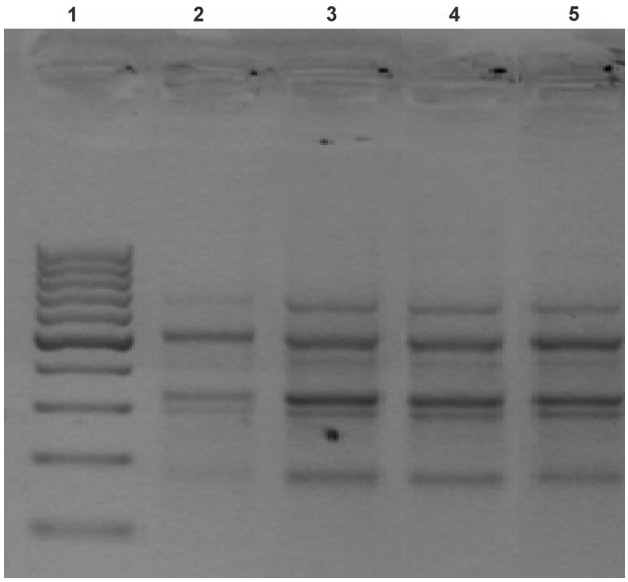

Fig. 8 PCR–RAPD pattern band using primer OPC-11 in *Drosophila melanogaster 1*. 100 bp DNA molecular marker (Promega), RAPD profiles from *2*. untreated DNA extract, *3*. DNA extract treated with immobilized RNase A from the 0.2 wt% RNase A concentration MAPLE target, *4*. DNA extract treated with immobilized RNase A from the 0.5 wt% RNase A concentration MAPLE target, *5*. DNA extract treated with immobilized RNase A from the 1 wt% RNase A concentration MAPLE target

quantitatively determine RNase A enzymatic activity. The ratio decreased after the treatment of the DNA extracts with the immobilized enzyme (Table 1) both for genomic DNA isolated from plants as well as animals, indicating RNA removal from the DNA extracts even for the sample obtained from MAPLE targets containing lower, 0.5 wt% RNase A concentration. Moreover, the difference between A_{260}/A_{280} ratios before and after treatment of DNA solutions with immobilized RNase A increase with the increase of the enzyme concentration in the MAPLE targets from 0.5 to 1 wt%. In case of the samples obtained from the lowest, 0.2 wt% RNase A concentration MAPLE target the determination of enzymatic activity is not sufficiently accurate. The final enzyme solution collected from the target holder after the laser immobilization experiments showed also enzymatic activity, but reduced as compared to the initial solution indicating that freezing and laser irradiation affect until certain extent the enzymatic activity of the RNase A base material. The difference between A_{260}/A_{280} ratios before and after treatment of DNA solutions with immobilized RNase A cannot be compared to the corresponding initial and final MAPLE solutions. This is due to the fact that the quantity of RNase A immobilized on the substrates surface remains always below the amount of the enzyme in the solutions. However, we would like to recall that the immobilized enzyme quantity can be easily controlled during the MAPLE process through the number of subsequent laser pulses.

RAPD reactions were performed to check the functional properties of DNA solutions treated with laser immobilized RNase A. RAPD is a PCR-based method, frequently used in molecular genetics for quantification of the genetic diversity at DNA level, based on the accuracy of the DNA fragment patterns. More defined and clear fragment patterns were obtained for the DNA extracts treated with immobilized RNase A (patterns 3–5 in Fig. 8) as compared to the untreated DNA extract solutions (pattern 2 in Fig. 8). This result demonstrates that RNA decontamination effectively takes place and the DNA extract solutions preserve their functional properties during their treatment with laser immobilized RNase A.

Conclusion

RNase A enzyme was immobilized on glass substrates by MAPLE technique. At enzyme concentrations below 0.5 wt% in the composite MAPLE targets discontinuous structures in form of droplets and rods, were obtained. The increase of the enzyme concentration to 1 wt% led to the formation of a continuous thin film on the substrate surface. Functional tests demonstrate that RNase A maintained its enzymatic activity during the laser immobilization process. The main advantage of the used laser technique relies in its sequential nature, offering the possibility to control the amount of immobilized material on the surface of the substrate through the number of the consecutive laser pulses. Moreover, laser deposition processes are simple, one-step procedures and the immobilization can be performed on any type of substrate materials. Immersion of immobilized RNase A in a DNA extract solutions reduced RNA contamination from DNA extracts, regardless of the DNA origin (animal and vegetal). The preservation of the RNase A enzymatic properties after immobilization on solid surfaces might be of great interest also for therapeutic purposes, since RNase enzymes are therapeutic biomaterials. RNA degradation is related to important biological processes like wound healing and carcinogenesis.

Acknowledgements The authors acknowledge with thanks the financial support of the Executive Unit for Financing Higher Education, Research, Development, and Innovation of the Romanian Ministry of Education, Research, Youth, and Sports under the Grant PN-II-RU-PD-2011-3-0241 and PN-II-PT-PCCA-2011-3.2-1235.

References

1. Raines RT (1998) Ribonuclease A. Chem Rev 98:1045–1066
2. Cuchillo CM, Nogués MV, Raines RT (2011) Bovine pancreatic ribonuclease: fifty years of the first enzymatic reaction mechanism. Biochemistry 50:7835–7842

3. Marshall GR, Feng JA, Kuster DJ (2008) Back to the future: ribonuclease A. Biopolymers 90:259–277
4. Dickson KA, Haigis MC, Raines RT (2005) Ribonuclease inhibitor: structure and function. Prog Nucleic Acid Res 80:349–374
5. Leland PA, Staniszewski KE, Kim BM, Raines RT (2001) Endowing human pancreatic ribonuclease with toxicity for cancer cells. J Biol Chem 276:43095–43102
6. Oldham RK, Dillman RO (eds) (2009) Principles of cancer biotherapy, 5th edn. Springer, Dordrecht
7. Dickson KA, Kang DK, Kwon YS, Kim JC, Leland PA, Kim BM, Chang SI, Raines RT (2009) Ribonuclease inhibitor regulates neovascularization by human angiogenin. Biochemistry 48:3804–3806
8. Gamble C, Trotard M, Seyec JL, Abreu-Guerniou V, Gernigon N, Berrée F, Carboni B, Felden B, Gillet R (2009) Antiviral effect of ribonuclease conjugated oligodeoxynucleotides targeting the IRES RNA of the hepatitis C virus. Bioorg Med Chem Lett 19:3581–3585
9. Rudolph B, Podschun R, Sahly H, Schubert S, Schröder JM, Harder J (2006) Identification of RNase 8 as a novel human antimicrobial protein. Antimicrob Agents Chemother 50:3194–3196
10. Teoli D, Parisi L, Realdon N, Guglielmi M, Rosato A, Morpurgo M (2006) Wet sol–gel derived silica for controlled release of proteins. J Control Release 116:295–303
11. Brook MA, Chen Y, Zhang Z, Brennan JD (2004) Sugar-modified silanes: precursors for silica monoliths. J Mater Chem 14:1469–1479
12. Cullen SP, Liu X, Mandel IC, Himpsel FJ, Gopalan P (2008) Polymeric brushes as functional templates for immobilizing Ribonuclease A: study of binding kinetics and activity. Langmuir 24:913–920
13. Zelikin AN (2010) Drug releasing polymer thin films: new era of surface-mediated drug delivery. ACS Nano 4:2494–2509
14. Shmueli RB, Anderson DG, Green JJ (2010) Electrostatic surface modifications to improve gene delivery. Expert Opin Drug Deliv 7:535–550
15. Jewell CM, Fuchs SM, Flessner RM, Raines RT, Lynn DM (2007) Multilayered films fabricated from an oligoarginine-conjugated protein promote efficient surface-mediated protein transduction. Biomacromolecules 8:857–863
16. Klibanov AM (1983) Immobilized enzymes and cells as practical catalysts. Science 219:722–729
17. Chrisey DB, Piqué A, Mcgill RA, Horwitz JS, Ringeisen BR, Bubb DM, Wu PK (2003) Laser deposition of polymer and biomaterial films. Chem Rev 103:553–576
18. Piqué A (2011) The matrix-assisted pulsed laser evaporation (MAPLE) process: origins and future directions. Appl Phys A 105:517–528
19. Eason R (ed) (2007) Pulsed laser deposition of thin films: applications-led growth of functional materials. Wiley, Hoboken
20. György E, Pérez del Pino A, Sauthier G, Figueras A (2009) Biomolecular papain thin films grown by matrix assisted and conventional pulsed laser deposition: a comparative study. J Appl Phys 106:11470
21. Smausz T, Megyeri G, Kékesi R, Vass Cs, György E, Sima F, Mihailescu IN, Hopp B (2009) Comparative study on pulsed laser deposition and matrix assisted pulsed laser evaporation of urease thin films. Thin Solid Films 517:4299–4302
22. György E, Axente E, Mihailescu IN, Predoi D, Ciuca S, Neamtu J (2008) Creatinine biomaterial thin films grown by laser techniques. J Mater Sci Mater Med 19:1335–1339
23. György E, Sima F, Mihailescu IN, Smausz T, Megyeri G, Kékesi R, Hopp B, Zdrentu LE, Petrescu SM (2009) Immobilization of urease by laser techniques: synthesis and application to urea biosensors. J Biomed Mater Res A 89:186–191
24. György E, Sima F, Mihailescu IN, Smausz T, Hopp B, Predoi D, Zdrentu LE, Petrescu SM (2010) Biomolecular urease thin films grown by laser techniques for blood diagnostic applications. J Mater Eng C 30:537–541
25. Popescu C, Roqueta J, Pérez del Pino A, Moussaoui M, Nogués MV, György E (2011) Processing and immobilization of enzyme Ribonuclease A through laser irradiation. J Mater Res 26:815–821
26. György E, Perez del Pino A, Roqueta J, Ballesteros B, Miguel AS, Maycock C, Oliva AG (2012) Synthesis and characterization of CdSe/ZnS core–shell quantum dots immobilized on solid substrates through laser irradiation. Phys Status Solidi A 209:2201–2207
27. György E, Perez del Pino A, Roqueta J, Ballesteros B, Miguel AS, Maycock CD, Oliva AG (2011) Synthesis and laser immobilization onto solid substrates of CdSe/ZnS core-shell quantum dots. J Phys Chem C 115:15210–15216
28. Hunter CN, Check MH, Bultman JE, Voevodin AA (2008) Development of matrix-assisted pulsed laser evaporation (MAPLE) for deposition of disperse films of carbon nanoparticles and gold/nanoparticle composite films. Surf Coat Technol 203:300–306
29. Neault JF, Diamantoglou S, Beauregard M, Nafisi S, Tajmir-Riahi HA (2008) Protein unfolding in drug-RNase complexes. J Biomol Struct Dyn 25:387–394
30. Georg H, Wharton CW, Siebert F (1999) Temperature induced protein unfolding and folding of RNase A studied by time-resolved infrared spectroscopy. Laser Chem 19:233–235
31. Kong J, Yu S (2007) Fourier transform infrared spectroscopic analysis of protein secondary structures. Acta Biochim Biophys Sin 39:549–559
32. Kieleczawa J (2006) DNA sequencing II: optimizing preparation and cleanup. Jones and Bartlett Publishers, Sudbury